Electronic Supplementary Information

Penetrative DNA Intercalation and G-Base Selectivity of an Organometallic Tetrahydroanthracene Ru^{II} Anticancer Complex

Hong-Ke Liu, John A. Parkinson, Juraj Bella, Fuyi Wang and Peter J. Sadler

Experimental

Reactions of II with ^{15}N-1.
HPLC
HPLC-ESI-MS
pH Measurements
NMR Spectroscopy.

Tables

Table S1 Negative ions detected by HPLC-ESI-MS for reaction mixture of [(η^6-tha)RuCl(en)]PF_6 (**1**) with ss-DNA **I** or duplex **II**.

Table S2 ^{1}H and ^{31}P NMR chemical shifts for DNA duplex **II** (at 283 K).

Table S3 ^{1}H and ^{31}P NMR chemical shifts for the product Ru-**II**a **(II**-Ru-G^3**)** in the 1.1:1 **1/II** reaction mixture. (283 K; Ru = {(η^6-tha)Ru(en)}$^{2+}$, **1′**).

Table S4 ^{1}H and ^{31}P NMR chemical shifts for product Ru-**II**b (**II**-Ru-G^6) in the 1.1:1 reaction **1/II** mixture (283 K; Ru = {(η^6-tha)Ru(en)}$^{2+}$, **1′**).

Table S5 Chemical shifts of en-NH protons of **1′** in different ruthenated adducts

Table S6 Intermolecular NOEs between arene and en-NH protons of **1′** and DNA protons in the **II**-Ru-G^3 adduct.

Table S7 Intermolecular NOEs between arene and en-NH protons of **1′** and DNA protons in the **II**-Ru-G^6 adduct.

Figures

Figure S1 800 MHz ^{1}H NMR spectra of the imino and aromatic region for A) duplex d(CGGCCG)$_2$ (**II**), B) the 1.1:1 **1/II** mixture, C) the 2:1 **1/II** mixture, and D) the 3:1 **1/II** mixture of duplex **II** and complex **1** in 90% H_2O/10% D_2O at 283 K, 0.34 M in 0.1 M $NaClO_4$ at pH 7.0. Assignments of DNA imino resonances (13-13.5 ppm) are indicated. Broadening of resonances and the appearance of new peaks in B, C and D are due to the ruthenation of duplex **II**. The decrease in the intensity of the imino peaks when the duplex is ruthenated by the second mol equivalent of **1** (spectrum C) suggests a decrease in imino proton residence time within the base pairs indicative of base-pair destabilization. The lifetime of the NH protons in the base pairs is further reduced when the duplex is ruthenated by the third mol equivalent of **1** (D). The assignments of peaks G^3* and G^6* to two mono-ruthenated duplexes are based on 2D correlation experiments (shown in Figure 5, see also Tables S2-4).

Figure S2 800 MHz 2D [^{1}H, ^{1}H] NOE NMR spectrum of the imino region for the 1.1:1 **1/II** mixture of duplex **II** and complex **1** in 90% H_2O/10% D_2O at 283 K, 0.34 M in 0.1 M $NaClO_4$ at pH 7.0. G^3* is the ruthenated G^3 base in mono-ruthenated duplex **II**-Ru-G^3, G^9H1 (G^3*) is the G^9H1 resonance in mono-ruthenated duplex **II**-Ru-G^3; G^6* is the ruthenated G^6 base in mono-ruthenated duplex **II**-Ru-G^6, G^2H1 (G^6*) is the G^2H1 resonance in mono-ruthenated duplex **II**-Ru-G^6.

Figure S3 2D [^{1}H, ^{15}N] HSQC NMR spectrum of a 1.1:1 **1/II** mixture of duplex **II** and ^{15}N-**1** (0.34 mM, 0.1 M $NaClO_4$ at 283 K, pH 7.0) in 90% H_2O/10% D_2O. Assignments for both en-NH(d) and NH(u) resonances of the unreacted ^{15}N-**1** (chlorido complex Cl-**1**) and en-NH(u) resonances of ruthenated duplex are shown. Assignments: a, en-NH(u) resonances of **II**-Ru-G^3 and **II**-Ru-G^6; b, not assigned. The en NH(d) resonances of both **II**-Ru-G^3 and **II**-Ru-G^6 were not observed. Ru = $\{(\eta^6\text{-tha})\text{Ru(en)}\}^{2+}$. For atom labels and structures of **II**-Ru-G^3 and **II**-Ru-G^6, see Figure 1 and Scheme 1.

Figure S4. Chemical-shift differences for NMR resonances of mono (G3*) ruthenated compared to unruthenated duplex. Chemical shift differences, $\Delta\delta$, measured as (δ**II*** - δ**II**) for a) aromatic, and b) H1′ resonances. Shift changes are indicated for the ruthenated 5′-CGGCCG-3′ strand (■) and for the complementary 3′-GCCGGC-5′ strand (▽).

Figure S5 Chemical-shift differences for NMR resonances of mono (G^6*) ruthenated compared to unruthenated duplex. Chemical shift differences, $\Delta\delta$, measured as (δ**II*** - δ**II**) for a) aromatic and b) H1′ resonances. Shift changes are indicated for the ruthenated 5′-CGGCCG-3′ strand (■) and for the complementary 3′-GCCGGC-5′ strand (▽).

Figure S6 2D [^{1}H, ^{1}H] ^{15}N-edited NOESY NMR spectrum of the 1.1:1 **1/II** mixture of duplex **II** and ^{15}N-**1** (0.34 mM, 0.1 M $NaClO_4$, 90% H_2O/10% D_2O, 283 K, mixing time 400 ms) showing NOE connectivities between the H resonances of en-^{15}NH of bound ruthenium fragment {^{15}N-(η^6-tha)Ru(en)}$^{2+}$ (^{15}N-**1′**) and the GH8 resonances of the two mono-ruthenated products **II**-Ru-G^3 and **II**-Ru-G^6. Both en-NHd resonances of ^{15}N-**1′** in both **II**-Ru-G^3 and **II**-Ru-G^6 were observed. For atom labels, see Figure 1.

Figure S7. 2D [^{1}H, ^{1}H] ^{15}N-edited TOCSY NMR spectrum of the 1.1:1 **1/II** mixture of duplex **II** and ^{15}N-**1** (0.34 mM, 0.1 M $NaClO_4$, 90% H_2O/10% D_2O, 283 K, mixing time 80 ms) showing cross-peaks for unreacted chlorido complex ^{15}N-**1**. For atom labels, see Figure 1.

Experimental

Reactions of II with ^{15}N-1. **^{15}N-1** (47 μL, 4.0 mM) was added into an NMR tube containing **II** (500 μL, 0.34 mM, 90% H_2O/10% D_2O); the final concentration of **II** was 0.31 mM, and the pH of the solutions was adjusted to 7.00. Dioxane was added as an internal ^{1}H NMR reference. The 1.1:1 **1/II** mixture was shaken for several minutes and kept at 298 K for 24 h in the dark. The ruthenations were monitored by both 1D ^{1}H NMR and by HPLC, and characterized by 2D [^{1}H, ^{1}H] TOCSY, ROESY and NOESY, 2D ^{15}N-decoupled [^{1}H, ^{15}N] and [^{1}H, ^{31}P] HSQC and 2D ^{15}N-edited TOCSY and NOESY NMR data. A further equimolar quantity of **^{15}N-1** (38 μL, 4.0 mM) was added into the above NMR tube containing the 1.1:1 **1/II** mixture, and the resulting 2:1 **1/II** mixture was kept at 298 K for 48 h in the dark. Ruthenation of the monoruthenated duplexes **II**-Ru-G^3 and **II**-Ru-G^6 by one equimolar amount of **^{15}N-1** was monitored by 1D ^{1}H NMR and by HPLC, and characterized by ^{15}N-decoupled 2D [^{1}H, ^{1}H] TOCSY and NOESY NMR data. An equimolar amount of **^{15}N-1** (42 μL, 4.0 mM) was added into the NMR tube containing the 2:1 **1/II** mixture, and the resulting 3:1 **1/II** mixture was also kept at 298 K for 48 h in the dark. Ruthenation of the diruthenated duplexes by **^{15}N-1** was monitored by 1D ^{1}H NMR and by HPLC, and also characterized by ^{15}N-decoupled 2D [^{1}H, ^{1}H] TOCSY and NOESY NMR data.

High Performance Liquid Chromatography (HPLC). A Hewlett-Packard Series 1100 quaternary pump and a Rheodyne sample injector with 100 μL and 500 μL loops, a HP 1100 series UV-Vis detector and HP 1100 series Chemstation with a HP enhanced integrator were used. Analytical separations for reaction mixtures of ruthenium complexes with DNA were carried out on a ACE300-5C8 reversed-phase column (250 × 4.6 mm, 300 Å, 5 μm, Hichrom Ltd) with detection at 260 nm. Mobile phases were A: 20 mM TEAA (in water, purified using a Millipore Elix 5 system), and B: 20 mM TEAA in acetonitrile. For analytical assays, the

flow rate was 1.0 mL min^{-1}. A 35-min linear gradient from 2.0% to 60% B was applied for all reaction mixtures of complex **1**.

HPLC-electrospray ionisation mass spectrometry (HPLC-ESI-MS). Negative-ion electrospray ionisation mass spectra were obtained with a Platform II mass spectrometer (Micromass, Manchester, U.K.) interfaced with a Waters 2690 HPLC system. The gradient described above was applied to an analytical ACE-5 column with a flow rate of 1.0 mL min^{-1} and a splitting ratio of 1/6. The spray voltage and the cone voltages were 3.50 kV and 40 V, respectively. The capillary temperature was 413 K with a 450 L h^{-1} flow of nitrogen drying gas. The quadrupole analyser, operated at a background pressure of 2×10^{-5} Torr, was scanned at 950 Da s^{-1}. Data were collected and analysed on a Mass Lynx (ver. 2.3) Windows NT PC data system using the Max Ent Electrospray software algorithm and calibrated versus an NaI calibration file.

NMR Spectroscopy. NMR data were acquired on 800 MHz or 600 MHz Bruker Avance NMR spectrometers at 278, 283, 288 and 298 K using dioxane as the inner reference (δ = 3.767, 298 K). NMR spectra for samples of ^{15}N-**1**, **II** and the reaction mixtures of ^{15}N-**1** with **II**, were recorded as follows. One-dimensional ^{1}H NMR spectra were typically acquired with 256 or 1 k transients into 16 k data points over a spectral width of 20 kHz by using a double-pulsed-field-gradient-spin-echo (DPFGSE) pulse sequence.[1] Two-dimensional ^{15}N-decoupled [^{1}H, ^{15}N] and [^{1}H, ^{31}P] HSQC NMR data sets were acquired and processed according to previously reported methods.[2-5] Two-dimensional ^{15}N-decoupled NOESY NMR data sets were acquired with 36 to 64 transients over a ^{1}H spectrum width of 20 ppm into 4096 data points for each of 512 t_1 increments (TPPI) using mixing times of 100 ms or 400

ms in a mixed solvent of 90%H_2O with 10% D_2O. The solvent signals were suppressed by using a DPFGSE routine.[1] Two-dimensional ^{15}N-decoupled TOCSY NMR data sets were acquired with 24 to 64 transients over a ^{1}H spectral width of 10 ppm into 4096 data points for each of 512 t_1 increments (TPPI) using a mixing time of 60, 80, 100 or 120 ms. Two-dimensional ^{15}N-decoupled ROESY NMR data sets were acquired with 64 transients over a ^{1}H spectral width of 20 ppm into 2048 data points for each of 512 t_1 increments (TPPI) using a mixing time of 200 ms. Two-dimensional ^{15}N-edited TOCSY NMR data sets were acquired with 64 transients over a ^{1}H spectral width of 10 ppm in the ω_2 domain and 6 ppm in the ω_1 domain into 1024 data points for each of 128 t_1 increments (States-TPPI) using a mixing time of 80 ms. Two-dimensional ^{15}N-edited NOESY NMR data were acquired with 512 transients over a ^{1}H spectrum width of 10 ppm in the ω_2 domain and 5 ppm in the ω_1 domain into 1024 data points for each of 24 t_1 increments (States-TPPI) using mixing times of 150, 250 and 400 ms. Two-dimensional ^{15}N-decoupled [^{1}H, ^{31}P] HSQC NMR data were acquired with 64 or 256 transients over a ^{1}H spectral width of 12 ppm in the ω_2 domain and 2 ppm in the ω_1 domain into 1024 data points for each of 32 or 40 t_1 increments. The water peak in NOESY, TOCSY and ROESY experiments was suppressed by using a DPFGSE routine.[2-3] In all cases the ^{15}N transmitter was centred at –30 ppm and ^{15}N chemical shifts were referenced relative to $^{15}NH_4Cl$ (0 ppm) and ^{31}P resonances to 85% H_3PO_4 (external) at 0 ppm. All NMR data were processed using Xwin-nmr (Version 3.5, Bruker BioSpin Ltd). Data were processed using standard apodizing functions prior to Fourier transformation.

pH Measurements. All pH measurements were made using a Corning 240 pH meter equipped with an Aldrich micro combination electrode calibrated with Aldrich standard

buffer solutions of pH 4, 7 and 10. For NMR samples in 90 % H_2O/10 % D_2O, no correction has been applied for the effect of deuterium on the glass electrode.

Reference

1. T. L. Hwang, A. J. Shaka, *J. Magn. Reson. Ser. A* **1990**, *112*, 275.
2. H. K. Liu, F. Y. Wang, J. A. Parkinson, J. Bella, P. J. Sadler, *Chem. Eur. J.* **2006**, *12*, 6151.
3. H. K. Liu, S. J. Berners-Price, F. Y. Wang, J. A. Parkinson, J. J. Xu, J. Bella, P. J. Sadler, *Angew. Chem., Int. Ed.* **2006**, *45*, 8153.
4. H. M. Chen, J. A. Parkinson, R. E. Morris, P. J. Sadler, *J. Am. Chem. Soc.* **2003**, *125*, 173.
5. H. M. Chen, J. A. Parkinson, S. Parsons, R. A. Coxall, R. O. Gould, P. J. Sadler, *J. Am. Chem. Soc.* **2002**, *124*, 3064.

Table S1. Negative ions detected by HPLC-ESI-MS for reaction mixture of [(η^6-tha)RuCl(en)]$^+$ (**1**) with ss-DNA **I** or duplex **II**.

Reaction	RT[a] [min]	Obs (Calcd)[b] m/z	Ions
1Ru:1**I**[c,d]	13.00	896.2 (896.5)	{**I**}$^{2-}$
	18.34	1066.7 (1043.5)	{**I**-Ru-G^2}$^{2-}$
	19.65	1065.5 (1043.5)	{**I**-Ru-G^3}$^{2-}$
	23.24	1065.7 (1043.5)	{**I**-Ru-G^6}$^{2-}$
	24.24	1237.0 (1190.6)	{**I**-Ru$_2$}$^{2-}$
	27.74	1237.0 (1190.6)	{**I**-Ru$_2$}$^{2-}$
	30.12	1407.2 (896.5)	{**I**-Ru$_3$}$^{2-}$
2Ru:1**I**	24.24	1237.0 (1190.6)	{**I**-Ru$_2$}$^{2-}$
	27.74	1237.0 (1190.6)	{**I**-Ru$_2$}$^{2-}$
	30.12	1407.2 (1337.6)	{**I**-Ru$_3$}$^{2-}$
3Ru:1**I**	29.91	1407.2 (1337.6)	{**I**-Ru$_3$}$^{2-}$
1Ru:**II**[e]	13.07	896.2 (896.5)	{**I**}$^{2-}$
	19.53	1065.5 (1043.5)	{**I**-Ru-G^3}$^{2-}$
	23.20	1065.7 (1043.5)	{**I**-Ru-G^6}$^{2-}$
2Ru:**II**	13.20	896.2 (896.5)	{**I**}$^{2-}$ [c]
	19.65	1065.5 (1043.5)	{**I**-Ru-G^3}$^{2-}$ [d]
	23.24	1065.7 (1043.5)	{**I**-Ru-G^6}$^{2-}$
	24.24	1237.0 (1190.6)	{**I**-Ru$_2$}$^{2-}$
	27.74	1237.0 (1190.6)	{**I**-Ru$_2$}$^{2-}$

[a] RT is the HPLC retention time (Figure 2). [b] Observed (Obs) and calculated (Calcd) mass-to-charge ratios for the observed ions. [c] **I** = CGGCCG. [d] for chemical structures, see Figure 1. [e] the unreacted duplex and the ruthenated duplex denatured to single-strand **I** and **I**-Ru during HPLC separation.

Table S2. ^{1}H and ^{31}P NMR chemical shifts for DNA duplex **II** (at 283 K).[1]

Residue	Proton									
	H8	H6	H5	H1'	H2'	H2"	H3'	H4'	imino	^{31}P	H41/H42
C^{1}/C^{7}		7.66	5.96	5.78	1.95	2.42	4.74	4.09			4.88/4.07
G^{2}/G^{8}	8.01			5.58	2.79	2.79	5.03	4.36	13.15	-1.01	
G^{3}/G^{9}	7.90			6.03	2.70	2.79	5.07	4.50	13.35	-0.88	
C^{4}/C^{10}		7.45	5.42	6.03	2.10	2.49	4.88	4.25		-1.18	7.15/8.79
C^{5}/C^{11}		7.53	5.72	5.65	2.07	2.39	4.88	4.14		-1.10	6.51/8.31
G^{6}/G^{12}	8.02			6.24	2.70	2.42	4.74	4.25	13.15	-0.74	

1. S. L. Lam, S. C. F. AuYeung, *J. Mol. Biol.* **1997,** *266*, 745-760.

Table S3. ^{1}H and ^{31}P NMR chemical shifts for the product Ru-**II**a (**II**-Ru-G^{3}) in the 1.1:1 **1/II** reaction mixture. (283 K; Ru = {(η^6-tha)Ru(en)}$^{2+}$, **1′**).

Residue[a]	δ/Proton[b] ($\Delta\delta$)[c]										
	H8	H6	H5	H1'	H2'	H2''	H3'	H4'	imino	H41/ H42	^{31}P
C^{1}		7.59 (-0.07)	5.89 (-0.07)	5.74	1.86 (-0.09)	2.41	4.73	4.09			---
G^{2}	8.35 (0.34)			6.3 (0.75)	2.49 (-0.30)	2.49 (-0.30)	5.03	4.36	13.15		-1.01
G^{3}	8.49 (0.59)			6.33 (0.30)	2.93 (0.26)	3.16 (0.37)	5.05	na[d]	13.39 (0.04)		-0.87
C^{4}		7.85 (0.40)	5.86 (0.44)	6.14 (0.11)	2.31 (0.21)	2.66 (0.17)	4.87	na		6.15 /8.03	-1.09 (0.09)
C^{5}		7.69 (0.16)	5.61 (-0.11)	6.08 (0.43)	2.30 (0.23)	2.49 (0.10)	na	na		7.04 /8.72	-1.13
G^{6}	7.95 (-0.07)			6.20	2.66	2.37 (-0.05)	4.74	4.24	13.11 (-0.04)		-0.74
C^{7}		7.61 (-0.05)	5.90 (-0.06)	5.74	1.89 (-0.07)	2.34	4.73	4.07			
G^{8}	7.97			5.56	2.76	2.76	5.03	4.35	13.11 (-0.04)		-1.01
G^{9}	7.88			6.10 (0.07)	2.66	2.84 (0.05)	5.09	4.47	13.49 (0.14)		-0.90
C^{10}		7.42	5.46	6.11 (0.08)	2.06	2.40 (-0.09)	4.89	4.45		6.38/ 8.20	-1.15
C^{11}		7.69 (0.16)	5.61 (-0.11)	6.07 (0.43)	2.30 (0.23)	2.46 (0.07)	na	na			-1.13
G^{12}	8.02			6.14 (-0.10)	2.66	2.31 (-0.11)	4.74	4.24	13.11 (-0.04)		-0.74

[a b] For DNA sequence and atom labels, see Figure 1. [c] $\Delta\delta$ values in brackets are chemical shift changes from free **II** (see Table S2) of $\geq$ 0.04 ppm [$\Delta\delta$ = δ(Ru-**II**a) - δ(**II**)]. [d] na = not assigned.

Table S4. ^{1}H and ^{31}P NMR chemical shifts for product Ru-**II**b (**II**-Ru-G^{6}) in the 1.1:1 reaction **1/II** mixture (283 K; Ru = {(η^{6}-tha)Ru(en)}$^{2+}$, **1′**).

Residue[a]	δ/Proton[b] ($\Delta\delta$)[c]										
	H8	H6	H5	H1'	H2'	H2''	H3'	H4'	imino	H41/H42	^{31}P
C^{1}		7.61 -(0.05)	5.90 (-0.06)	5.74	1.89 (-0.06)	2.39	4.73	4.09			
G^{2}	7.98			5.54	2.76	2.76	5.03	4.35	13.11 (-0.04)		-1.01
G^{3}	7.88			5.98 (-0.05)	2.67	2.75	5.07	4.49	13.32		-0.90
C^{4}		7.42	5.38	5.99	2.07	2.45	4.89	4.46		7.07/8.77	-1.15
C^{5}		7.83 (0.30)	6.04 (0.32)	5.99 (0.34)	2.28 (0.21)	2.66 (0.27)	na[d]	na		6.72/8.56	na
G^{6}	8.48 (0.46)			6.33 (0.09)	2.69	2.49 (0.07)	na	4.23	13.04 (-0.11)		-0.79 (-0.05)
C^{7}		7.77 (0.11)	5.80 (-0.16)	6.15 (0.37)	2.12 (0.17)	2.37 (-0.05)	na	na			
G^{8}	8.04			6.14 (0.56)	2.76	2.76	5.03	na	13.15?		-1.01
G^{9}	7.88			6.10 (0.07)	2.66	2.84 (0.05)	5.09	4.49	13.36		-0.90
C^{10}		7.42	5.38	5.99	2.06	2.45	4.89	4.46		7.11 /8.76	-1.15
C^{11}		7.49	5.69	5.60	2.03	2.34	na	na		6.48 /8.26	-1.13
G^{12}	7.98			6.19	2.66	2.38	4.74	4.24	13.11 (-0.04)		-0.74

[a b] For DNA sequence and atom labels, see Figure 1. [c] $\Delta\delta$ values in brackets are chemical shift changes from free **II** (see Table S2) of $\geq$ 0.04 ppm [$\Delta\delta$ = δ(Ru-**II**b)- δ(**II**)]. [d] na = not assigned.

Table S5. Chemical shifts of en-NH protons of **1** in different ruthenated adducts.

Adduct	T/*K*	□δ NHd	□δ NHu
II-Ru-G[3], **II**-Ru-G[6], **1′**[a]	288	3.86/3.95[b]	6.47/6.56
		(-28.90)	(-28.90)
[(η^6-tha)Ru(en)Cl]$^+$	288	3.67(-23.38)	6.24(-23.38)
[(η^6-tha)Ru(en)(H_2O)]$^{2+}$	288	4.04(-23.68)	6.06(-23.68)
[(η^6-tha)Ru($^{15}N_2$-en)(9EtG-*N*7)]$^{2+}$	310	broad[c] (-29.38)	6.40(-29.38)
	283	3.85[d] (-29.35)	6.50(-29.35)
		6.0[d] (-29.74)	6.43(-29.74)
	274	3.89 (29.40)	6.55 (29.40)
		6.05 (-29.92)	6.45(-29.92)
[(η^6-tha)Ru($^{15}N_2$-en)(5'-GMP-*N7*)]$^{2+}$	328	broad[c] (-28.50)	6.19(-28.50)
	308	broad[c] (-27.92)	6.25(-27.89)
		broad[c] (-29.28)	6.27(-29.28)
	278	broad[c] (-27.89)	6.25(-27.89)
		broad[c] (-29.28)	6.27(-29.28)

[a] One pair (labelled **1′**) was identified on the basis of NOESY NHu-NHd cross-peaks in the mixture of mono-ruthenated adducts, but only one broad cross-peak was detected at 6.52/-28.90 ppm in the 2D ^{15}N-decoupled [^{1}H, ^{15}N] HSQC spectrum, assignable to **1**-NHu. The assignment of en-NH_2 protons as 'u' or 'd' (Scheme 1) is based on previous work (H. Chen, J. A. Parkinson, S. Parsons, R. A. Coxall, R. O. Gould, P. J. Sadler, *J. Am. Chem. Soc.* **2002**, *124*, 3064). [b] This assignment is based on a NOESY experiment. [c] Too broad to observe. [d] Signal is broad and weak.

Table S6. Intermolecular NOEs between arene and en-NH protons of **1′** and DNA protons in the **II**-Ru-G^3 adduct[a].

Base	Proton	Connectivity[b]
G^3	H8	NHd (m, 2.92), H9,10 (w,4.73), NHu(w,3.95), H2, 3 (w,3.72), H1,4 (w,3.45)
	H1′	H9/10 (w), H1,4(w)
	H2′	H2,3(w, 3.81),H1,4 (m,2.91)
	H2″	H9,10(w, 4.36), H1,4(w, 3.37)
C^4	H6	H9,10 (w, 3.71), H1,4(w, 3.24)
	H5	H9,10 (w, 3.5), H2,3(w,3.72), H1,4(m, 2.93)
	H1'	H5,8(w, 3.60), H9,10 (w, 4.14)
G^9	H1′	H6,7 (w,3.67)
	H2'	H6,7 (w, 3.18)
	H2"[c]	H6,7 (m,2.51)
C^{10}	H6[d]	H6,7 (m,2.94)
	H5	H5,8 (w, 3.08)
	H1'	H6,7 (m, 2.69)
G^2	H8	NHd(w, 3.03), enCH2(m, 2.62)
	H2'	NHd (m,2.49)

[a] For atom labels and DNA sequence, see Figure 1. [b]Strength of NOEs: w = weak, m = medium, based on intensities of cross-peaks. The purple colour is the observed strength of NOEs.

Table S7. Intermolecular NOEs between arene and en-NH protons of **1** and DNA protons in the **II**-Ru-G^6 adduct[a].

Base	Proton	Connectivity[b]
G^6	H8	NHu (w, 3.66), H9,10 (m,2.86), NHd(w,3.40), H2, 3 (w,4.28), H1,4 (s,2.74)
	H1′	H9,10 (w,3.47), H5,8 (m,2.55)
	H4'	H9,10 (w,4.34), H5,8(m,4.24)
	H5'	H9,10 (w,4.47)
C^5	H6	H1,4(m,2.87)
	H5	H2,3(w,2.96), H1,4(w,3.47)
	H1'	H1,4(w,3.72)
	H2'	H1,4(m,2.60)
	H2"	H2,3(w,2.99), H1,4(m,2.72)
G^8	H1′	H6,7 (m,3.44), H5,8 (w, 3.50)
	H2'/H2"	H5,8 (w,3.85), H6,7 (w,3.89)
C^7	H1'	H6,7 (w,2.94)
	H2'	H6,7 (m,2.44)
	H2"	H6,7 (m,3.01), H5,8 (m,2.53)

[a] For atom labels and DNA sequence, see Figure 1. [b] Strength of NOEs: w = weak, m = medium, s = strong, based on intensities of cross-peaks. The purple colour is the observed strength of NOEs.

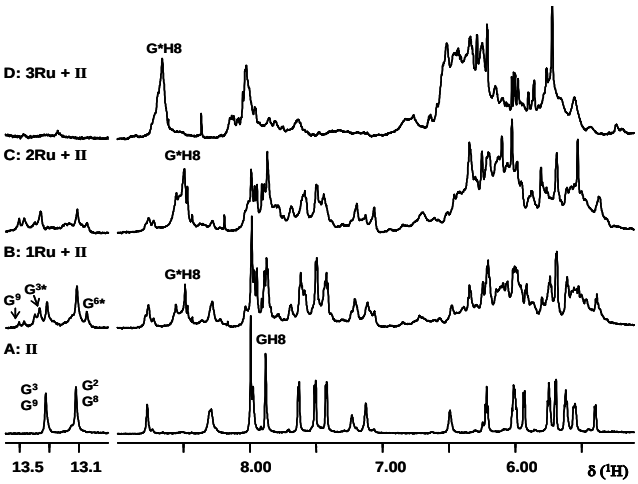

Figure S1 800 MHz ^{1}H NMR spectra of the imino and aromatic region for A) duplex d(CGGCCG)$_2$ (**II**), B) the 1.1:1 **1/II** mixture, C) the 2:1 **1/II** mixture, and D) the 3:1 **1/II** mixture of duplex **II** and complex **1** in 90% H_2O/10% D_2O at 283 K, 0.34 M in 0.1 M $NaClO_4$ at pH 7.0. Assignments of DNA imino resonances (13-13.5 ppm) are indicated. Broadening of resonances and the appearance of new peaks in B, C and D are due to the ruthenation of duplex **II**. The decrease in the intensity of the imino peaks when the duplex is ruthenated by the second mol equivalent of **1** (spectrum C) suggests a decrease in imino proton residence time within the base pairs indicative of base-pair destabilization. The lifetime of the NH protons in the base pairs is further reduced when the duplex is ruthenated by the third mol equivalent of **1** (D). The assignments of peaks G^3* and G^6* to two mono-ruthenated duplexes are based on 2D correlation experiments (shown in Figure 5, see also Tables S2-4).

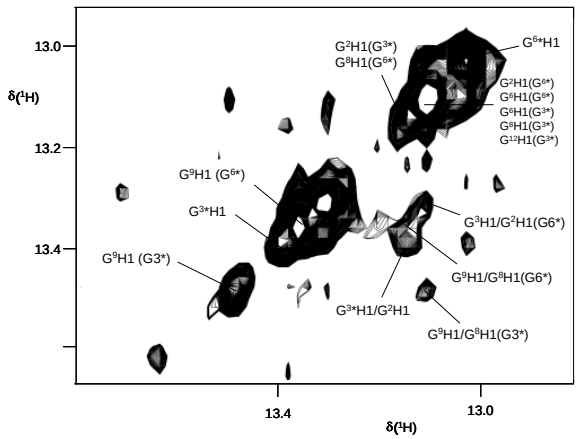

Figure S2. 800 MHz 2D [^{1}H, ^{1}H] NOE NMR spectrum of the imino region for the 1.1:1 **1/II** mixture of duplex **II** and complex **1** in 90% H_2O/10% D_2O at 283 K, 0.34 M in 0.1 M $NaClO_4$ at pH 7.0. G^3* is the ruthenated G^3 base in mono-ruthenated duplex **II**-Ru-G^3, G^9H1 (G^3*) is the G^9H1 resonance in mono-ruthenated duplex **II**-Ru-G^3; G^6* is the ruthenated G^6 base in mono-ruthenated duplex **II**-Ru-G^6, G^2H1 (G^6*) is the G^2H1 resonance in mono-ruthenated duplex **II**-Ru-G^6.

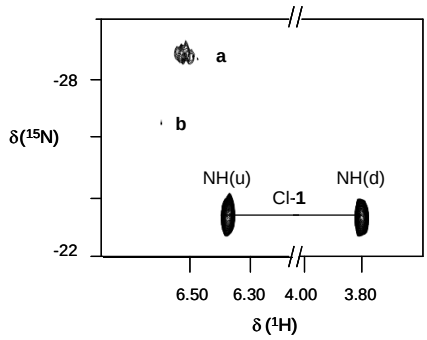

Figure S3. 2D [^{1}H, ^{15}N] HSQC NMR spectrum of a 1.1:1 **1/II** mixture of duplex **II** and ^{15}N-**1** (0.34 mM, 0.1 M $NaClO_4$ at 283 K, pH 7.0) in 90% H_2O/10% D_2O. Assignments for both en-NH(d) and NH(u) resonances of the unreacted ^{15}N-**1** (chlorido complex Cl-**1**) and en-NH(u) resonances of ruthenated duplex are shown. Assignments: a, en-NH(u) resonances of **II**-Ru-G^{3} and **II**-Ru-G^{6}; b, not assigned. The en NH(d) resonances of both **II**-Ru-G^{3} and **II**-Ru-G^{6} were not observed. Ru = {(η^{6}-tha)Ru(en)}$^{2+}$. For atom labels and structures of **II**-Ru-G^{3} and **II**-Ru-G^{6}, see Figure 1 and Scheme 1.

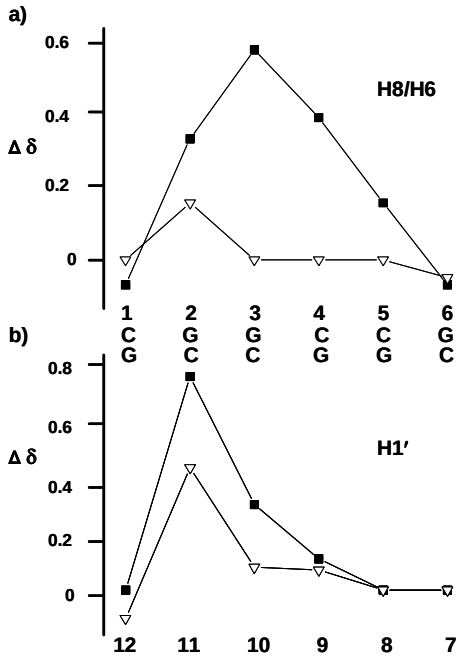

Figure S4. Chemical-shift differences for NMR resonances of mono (G3*) ruthenated compared to unruthenated duplex. Chemical shift differences, $\Delta\delta$, measured as (δ**II*** - δ**II**) for a) aromatic, and b) H1′ resonances. Shift changes are indicated for the ruthenated 5′-CGGCCG-3′ strand (■) and for the complementary 3′-GCCGGC-5′ strand (▽).

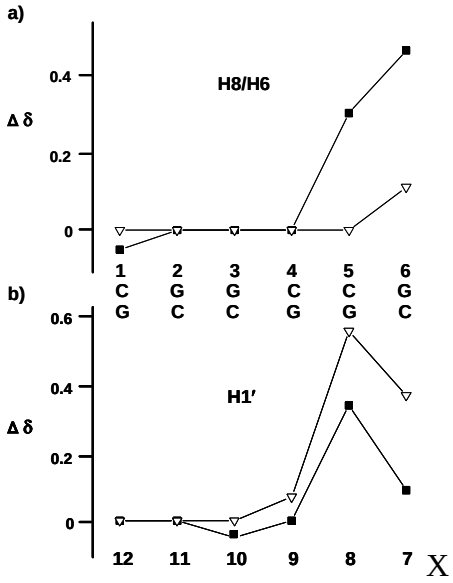

Figure S5 Chemical-shift differences for NMR resonances of mono (G^6*) ruthenated compared to unruthenated duplex. Chemical shift differences, $\Delta\delta$, measured as (δ**II*** - δ**II**) for a) aromatic and b) H1′ resonances. Shift changes are indicated for the ruthenated 5′-CGGCCG-3′ strand (■) and for the complementary 3′-GCCGGC-5′ strand (▽).

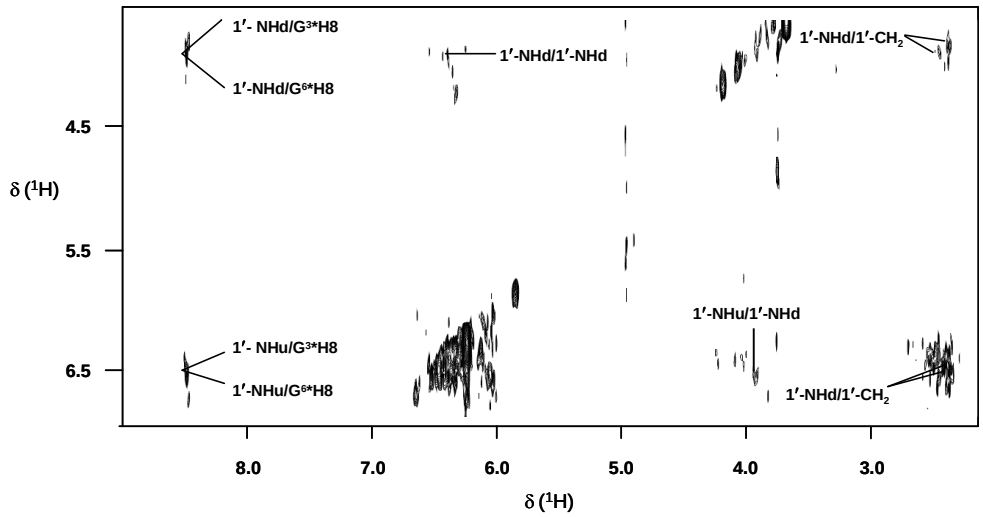

Figure S6. 2D [^{1}H, ^{1}H] ^{15}N-edited NOESY NMR spectrum of the 1.1:1 **1/II** mixture of duplex **II** and ^{15}N-**1** (0.34 mM, 0.1 M $NaClO_4$, 90% H_2O/10% D_2O, 283 K, mixing time 400 ms) showing NOE connectivities between the H resonances of en-^{15}NH of bound ruthenium fragment $\{^{15}N\text{-}(\eta^6\text{-tha})Ru(en)\}^{2+}$ (^{15}N-**1′**) and the GH8 resonances of the two mono-ruthenated products **II**-Ru-G^3 and **II**-Ru-G^6. Both en-NHd resonances of ^{15}N-**1′** in both **II**-Ru-G^3 and **II**-Ru-G^6 were observed. For atom labels, see Figure 1.

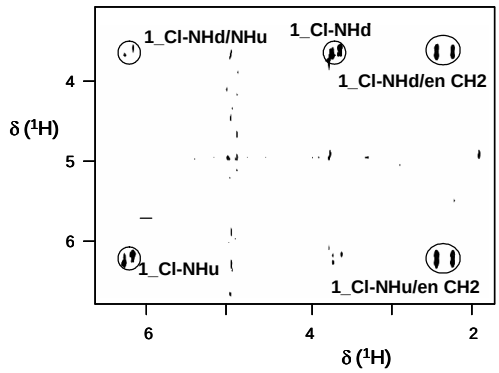

Figure S7. 2D [^{1}H, ^{1}H] ^{15}N-edited TOCSY NMR spectrum of the 1.1:1 **1/II** mixture of duplex **II** and ^{15}N-**1** (0.34 mM, 0.1 M $NaClO_4$, 90% H_2O/10% D_2O, 283 K, mixing time 80 ms) showing cross-peaks for unreacted chlorido complex ^{15}N-**1**. For atom labels, see Figure 1.